

1 **Are Detected Trends in Flood Magnitude and Shifts in the Timing of**
2 **Floods of A Major River Basin in India, Linked To Anthropogenic**
3 **Stressors?**

4 *Nandamuri Yamini Rama, Poulomi Ganguli*, Chandranath Chatterjee*

5 Department of Agricultural and Food Engineering, Indian Institute of Technology
6 Kharagpur, West Bengal 721 302, India

7 **Correspondence to: Dr. Poulomi Ganguli (pganguli@agfe.iitkgp.ac.in)*

8

9 **ABSTRACT**

10 Analyzing of trends in flood magnitude and the timing of the dates of flood occurrences of
11 large river basins across globe are essential for understanding changes in water availability
12 (high or low flows) and assessing fidelity of global hydrological models. Our research is
13 motivated by the recent six major consecutive floods in Mahanadi (years: 2001, 2003, 2006,
14 2008, 2011 and 2013) River Basin (MRB), which is one of the largest peninsular Rivers in
15 India with a catchment area of 14,1589 km². We examine the altered risk of flooding focusing
16 on changes in the flood regimes and a shift in the timing of floods over the past four decades
17 (1970-2016) using hydrometric observations across the MRB. A framework for identification
18 of flood regime changes is developed using monsoonal maxima peak discharge (MMPD) and
19 peak over threshold (POT) events at 24 stream gauges over the basin. We find a mix of
20 (insignificant) up/downward trends in flood magnitude at Upper MRB (Region I). On the
21 other hand, the middle reaches of the basin (Region II) showed an upward trend in flood
22 magnitude, with a larger number of sites detect significant trends in flood magnitude for the

23 POT events. Further, we find the downward trends in MMPD series at Region I is field
24 significant (at 10% significance level) whereas none of the trends in POT series show field
25 significance. Only a few stations detected abrupt changes in the flood time series, and they
26 are spatially clustered at Region I, whereas Region II showed no evidence of change points.
27 A delayed (or earlier) shift in flood timing is apparent for most of the sites, notwithstanding
28 the mean date of flood occurrence is in August irrespective of the type of flood series. The
29 outcomes of the study contribute to ensuring flood resilience at densely populated large river
30 basins.

31

32 **Keywords:** *Mahanadi River Basin, floods, trend analysis, change points, circular statistics.*

33

34 **1. Introduction**

35 Floods are one of the most commonly occurring natural calamities in India, with an estimated
36 average loss of US \$54.3 billion between 1953 and 2016 (Chandra, 2018). Although the
37 Intergovernmental Panel on Climate Change - Special Report on Extremes (Murray and Ebi,
38 2012) suggests there is a low agreement and hence low confidence regarding changes in the
39 magnitude or frequency of floods at the global scale, using ground-based observational
40 record, a recent study (Halgamuge and Nirmalathas, 2017) have indicated that there have
41 been a moderate increase in flood severity and the number of displaced people (~152k) owing
42 to floods in India during recent decades (1985-2016). With increasing temperature, the
43 frequency and magnitude of fluvial floods are expected to amplify in a warming climate
44 (Hirabayashi et al.; Stocker, 2013).

45 Analyzing changes in floods is vital in many hydrological applications, such as hydropower
46 production and developing flood risk management portfolios of structural and nonstructural
47 measures (Hall and Solomatine, 2008; Mirza, 2003; Rosner et al., 2014). Further, analyzing
48 temporal changes in flood series could lead to improved flood frequency estimates in a
49 nonstationary climate (Kwon et al., 2008; López and Francés, 2013; Villarini et al., 2009b;
50 Vogel et al., 2011). So far, several studies have analyzed temporal changes in flood
51 magnitude and flood seasonality over continental scales. Examples of recent studies include
52 but are not limited to (Petrow and Merz, 2009) throughout Germany (Cunderlik and Ouarda,
53 2009), Canada (Burn et al., 2016, 2010, and Burn and Whitfield, 2018), Europe (Blöschl et
54 al., 2017; Hall et al., 2014) and Scandinavia (Matti et al., 2017) and at a watershed scale,
55 Poyang Lake Basin, China (Tian et al., 2011), Mahanadi River basin, India (Jena et al., 2014
56 and Panda et al., 2013), and Athabasca River Basin, Canada (Bawden et al., 2014). Apart
57 from analyzing monotonic trends, a few studies (Nka et al., 2015; Villarini et al., 2009a) have
58 investigated abrupt change points to detect possible nonstationarities in the flood time series.
59 The details of the key literature, including modeling frameworks highlighting the main
60 findings, are summarized in Table 1.

61

62 To the best of our knowledge, so far most of the assessments have focused on analyzing flood
63 seasonality and associated flood regime changes over either North America (Burn et al.,
64 2016; Burn and Whitfield, 2018; Regonda et al., 2005) or Europe (Blöschl et al., 2017)
65 focusing over flood flow across nival and mixed flow regimes in mid-latitudes (35-55° N)
66 and high latitudes (> 60° N). However, most detrimental human impacts owing to floods

67 could be potentially from developing countries because of low flood protection strategies and
68 vulnerability of populations (Tessler et al., 2015).

69

70 To fill this research gap, this study contributes to a comprehensive understanding of trends
71 and flood seasonality of Mahanadi River Basin (MRB), one of the largest peninsular Rivers
72 in India covering tropical pluvial discharge regime (domain: 23.5°N – 23.5°S). Mahanadi is
73 one of the major peninsular rivers in India with the catchment area of 14,1589 km²
74 (occupying ~ 4.3% of total landmass in the country) and ranked second in the nation
75 concerning water potential and flood-producing capacity (National Institute of Hydrology,
76 2018). According to the 2011 Census, 23.09 Million people (76% urban and 23% rural)
77 resides (NIH, 2018) at MRB. Between 1985 and 2016 (within a span of 32 years), the MRB
78 has experienced 25-major flood events causing immense losses to life and property; out of
79 which 22 events were due to prolonged monsoon rainfall, extreme precipitation followed by
80 dam releases and only 3 of them were owing to tropical cyclones in the delta region
81 (Brakenridge, 2018). The historical records indicated the MRB had been subjected to severe
82 floods in recent past, i.e., 2001, 2003, 2006, 2008, 2011 and 2013 (Beura, 2015; Jena et al.,
83 2014). The frequency of occurrence of high floods in the MRB is increasing with an increase
84 in extreme rainfalls and loss of forest cover in the middle and lower reaches of the basin
85 (Dadhwal et al., 2010; Jena et al., 2014; Panda et al., 2013). On the other hand, the upper
86 reaches (above the delta region) experience minimum flooding because of control structures,
87 levees, and relatively steep slopes. A detection and attribution study (Mondal and Mujumdar,
88 2012) over basin-wide monsoon precipitation and streamflow at Hirakud reservoir have

89 shown a marked contribution of human-induced climate change to flow regimes rather than
90 the observed precipitation pattern across the MRB. Thus, understanding the basin-wide flood
91 regime shift at densely populated MRB holds great interest.

92

93 Given above challenges in flood flow characterizations and adaptations across MRB, this
94 study aims to examine following primary hypothesis: *Basin-wide floods and their attributes*
95 *across MRB have not shown any significant changes in severity, frequency, the timing of*
96 *occurrences and spatial coverage.*

97

98 To investigate further whether floods over MRB are becoming more frequent, we have
99 formulated the following set of research questions:

- 100 (i) What are the patterns of trends and abrupt changes in extreme flood magnitude across
101 MRB for the period 1970-2016?
- 102 (ii) What is the sensitivity of trends and flood seasonality to different flood samplings used
103 to define flood series?
- 104 (iii) Are the detected trends in flood magnitude sensitive to catchment morphology (i.e.,
105 watershed size and elevation)?
- 106 (iv) Is there any shift in timing of flood occurrences in a changing climate?

107

108 The paper is organized as follows: the study region, datasets used and the modeling
109 framework including the detailed workflow are described in Section 2. Section 3 discusses
110 the results. Finally, the discussion and the salient conclusions of the study are presented in

111 Section 4. The analyses are performed on entire MRB consisting of 24 stream gauge records.
112 The outcomes of the research are expected to provide a detailed understanding of the nature
113 of floods in the MRB in a present-day climate. Furthermore, the modeling framework can be
114 easily transferred to understand flood behavior in similar climatic regions and future climate
115 projections.

116

117 **2. Data and methods**

118 *2.1 Study Area and Data*

119 We selected entire MRB (80°30' to 86°50'E longitudes and 19°20' to 23°35'N latitudes)
120 covering the states of Chhattisgarh (52.42%) and Odisha (47.14%) and small portions in
121 Maharashtra (0.23%), Madhya Pradesh (0.11%) and Jharkhand (0.1%). Mahanadi River
122 originates in Dhamtari district of Chhattisgarh and drains into the Bay of Bengal, spanning a
123 total length of 851 km. The MRB is a rain-fed river with maximum precipitation observed
124 between July and the first half of September in general, and there is no significant
125 contribution from groundwater recharge. December and January are the coldest months in
126 the basin with the minimum temperature between 4°C to 12°C, and May is the hottest month
127 with a maximum temperature between 42°C to 45°C (CWC, 2014). Figure 1(a) shows the
128 spatial variability in elevation and stream gauge stations across the basin. Based on basin
129 morphology, the MRB is divided into three distinct regions namely (CWC, 2014):

130 a. Upper (Region I): Drainage area between the source and Hirakud dam also called
131 upper region. The area of this section is 84,700 km² out of which 75,136 km² lie in
132 Chhattisgarh state.

133 b. Middle (Region II): Drainage area between Hirakud dam and head of Delta also called
134 middle region. The area of this region is 50,745 km².

135 c. Lower (Region III): Drainage area between the head of delta and Bay of Bengal also
136 called Delta region (Orissa State Water Plan, 2004).

137 Approximately, 65% of the basin is upstream from the Hirakud dam (Dadhwal *et al.*, 2010).

138 The Hirakud dam is a multipurpose project intended for flood control, power generation, and

139 irrigation. It was built across the Mahanadi River, about 15 kilometers upstream from

140 Sambalpur town in the state of Odisha during 1957 with a catchment area of 83,400 km²

141 (85% of catchment area lying in Chhattisgarh). The dam has a live Storage Capacity of 4823

142 MCM and Spillway capacity of 42,450 cumecs. Figure 1(b) shows the district wise

143 population density highlighting major cities (Census data 2011) indicating population varies

144 between 1,232 and 40,63,870. The largest population is in Raipur (the state capital of

145 Chhattisgarh) followed by Durg and Bilaspur in Chhattisgarh state; Cuttack, Khordha, and

146 Sundargarh in Odisha state.

147

148 *2.2 Data Collection and Screening*

149 The daily streamflow discharge data of 43 gauge stations located in the study area between

150 1971 and 2016 were obtained from the Central Water Commission, Government of India. All

151 these stations have varying length of records; hence we have selected only those stations that

152 have at least 70% data availability during monsoon months (June to September) with a

153 minimum of 10 complete years of record. The pre-processing followed by the data screening

154 procedure led to the exclusion of 19 stations, and the resulting record contains 24 stations.

155 Table S1 provides the details of selected discharge gauge stations with a period of data
156 availability. All these gauge stations are located within geographical coordinates of 81°14' to
157 85°45' E longitudes and 20°05' to 23°12' N latitudes. The MRB was delineated using the
158 Shuttle Radar Topography Mission (SRTM) Digital Elevation Model of 90 m resolution
159 (Jarvis et al., 2008) using Arc GIS10.1 software. The basin has the maximum, and average
160 elevations of 1319 m and 376.2 m above mean sea level (MSL) respectively.

161

162 *2.3 Modelling Framework*

163 A detailed workflow of the research is shown in Figure 2. The two methods of sampling flood
164 events, namely monsoonal (June-September) maxima peak discharge (MMPD) and Peak
165 over Threshold (POT) events are presented, and the two perspectives of analyses are
166 discussed to characterize floods. Further, the Mann-Kendall trend test and Pettitt change
167 point tests are used to detect monotonic trends and abrupt changes in the time series. Trend
168 analyses were conducted both at '*local* (at-site)' and regional (collection of sites) level. The
169 magnitude of the trend slope was also determined to analyze changes in flood severity. Flood
170 seasonality and the shift in timing of occurrences of floods are explored using circular
171 statistics. In the subsequent section, we have described each of these modeling components:

172

- 173 • *Extraction of Monsoonal Maximum Peak Discharge (MMPD) Events and Peak over*
174 *Threshold (POT) Events*

175 The most common indicator of flood trends in rainfed basins in India is the monsoonal
176 maximum discharge events, i.e., the largest daily mean streamflow during monsoon (June to

177 September) months in each calendar year (1 January –31 December). The independent peak
178 flows during monsoon season (one event per year) were selected from daily mean streamflow
179 records of all the respective gauge stations. Few studies suggest (Burn et al., 2016; Svensson
180 et al., 2005), POT series gives more information about statistical attributes of extremes as
181 compared to the MMPD, revealing a better temporal pattern of flood occurrence. On the other
182 hand, selecting a suitable threshold value for extracting POT data is one of the challenging
183 aspects (Burn et al., 2016). Here, we checked various thresholds, ranging from 98 to 99.9th
184 percentiles at an interval of 0.5, and then finalized a threshold based on 98.5th percentile to
185 select on an average 3- peak discharge events per year. To ensure selected POT events are
186 independent of each other, following the literature (Petrov and Merz, 2009; Svensson et al.,
187 2005), we selected different time spans based on the catchment area of gauge stations, i.e., 5
188 days for catchment size <45,000 km² and 10 days for catchment size between 45,000 km²
189 and 100,000 km². In our study, about 80% of gauging stations have catchment areas less than
190 45,000 km², and the remaining 20% of gauging stations have catchment areas between 45,000
191 km² and 100,000 km². If two consecutive POT events occurred within the specified period,
192 the smaller event is dropped, and the higher event is adopted for the analysis.

193

194 • *Detection of monotonic trends and change points in peak discharge events*

195 In this study, the Mann–Kendall (Kendall, 1975; Mann, 1945) and the Pettitt (Pettitt, 1979)
196 tests are used to identify trends and change points in the peak discharge events. For all these
197 tests, the null hypothesis assumes that there is no trend or no change points in the peak
198 discharge events at selected significance levels. The rank-based Mann-Kendall (MK) test is

199 regarded as a robust nonparametric test (Kendall, 1975; Mann, 1945), and widely used for
200 examining trends in many hydroclimatic variables (Burn et al., 2016; Petrow and Merz,
201 2009), that are not necessarily normally distributed (Kunkel et al., 1999). However, the
202 presence of autocorrelations in a time series set can increase the expected number of false
203 positive outcomes for the Mann–Kendall test statistics (Storch et al., 1999). Therefore, trends
204 in MMPD and POT time series were evaluated using the modified Mann–Kendall trend test
205 with corrections for ties and auto-correlation (Hamed and Ramachandra Rao, 1998; Reddy
206 and Ganguli, 2013) at a 10% significance level. The magnitude of slope (change per unit
207 time) is estimated using the Theil-Sen Slope (Sen, 1968; Theil, 1950).

208

209 While the power of trend estimates at a gauge (or '*local*') level is assessed using standard
210 statistical significance tests available in the literature, the nature of trend at a regional level
211 is analyzed using field significance test. The field significance is evaluated using False
212 Discovery Rate (FDR) based approach (Benjamini and Hochberg, 1995; Benjamini and
213 Yekutieli, 2001), which has been compared to other methods and shown to be relatively
214 insensitive to spatial dependence among sites (Khaliq et al., 2009). The power of the field
215 significance test is evaluated at the same significance level as their locally identified trend.

216

217 The time series of flood series are tested for abrupt changes in means (i.e., average peak
218 discharge) by applying the Pettitt test for single change-point detection (Villarini et al., 2012).
219 When dealing with long historical data sets, the change-point analysis is preferred as it
220 provides point (or time) of change that has occurred in the time series with a statistical

221 significance level of the changes detected (Perreault et al., 2000; Rodionov, 2005; Villarini
222 et al., 2009a). We calculate the power of the statistical test at three significance levels of α
223 = 5%, 10%, and 15%. At $\alpha = 10\%$ significance level, only 3 and 2 out of 24 stations had a
224 change point for MMPD and POT events, respectively. Hence, we relaxed the significance
225 level up to $\alpha = 15\%$, to increase the power of the test. All three statistical tests described
226 here are nonparametric, which are robust to the presence of outlier and the length of the time
227 series.

228

229 • *Detection of Seasonality trends in peak discharge events*

230 The shift in seasonality of the flood series is detected using the directional or circular statistics
231 (Mardia, 1972; Pewsey et al., 2013), which is widely used method to define the timing (date
232 of occurrence) and the persistence of flood events (Burn et al., 2016; Cunderlik, 2004; Dhakal
233 et al., 2015; Tian et al., 2011). Laaha and Blöschl (2006) summarized the seasonality indices
234 and how they can be estimated based on the discharge time series. In this method, the date of
235 occurrence of a peak flow, as a directional statistic of time, is translated into location on the
236 circumference of a circle, with the mathematical convention that the start of the flood season
237 is shown at its most easterly point and time proceeds in a counter-clockwise direction (Fisher
238 1993; Mardia, 1972). Once individual dates of flood occurrences are expressed as a
239 directional variable, then directional mean and variance can be calculated.

240 The date of flood occurrence (*Julian Date*)_{*i*} can be converted to an angular value (θ_i), in
241 radians for an event "*i*" using:

242

$$\theta_i = (\text{Julian Date})_i \frac{2\pi}{\text{len yr}} \quad (1)$$

243

244 Where, *Julian Date* = 1 for 1 January and *Julian Date* = 365 for 31 December (or 366 for
245 leap year); *len yr* is the number of days in a year, i.e., 365 for a normal year and 366 for a
246 leap year.

247 For a sample of *n* events, the X - and Y -coordinates of the mean date can be determined as
248 (Burn and Whitfield, 2018)

249

$$\bar{X} = \frac{\sum_{i=1}^n q_i \cos \theta_i}{\sum_{i=1}^n q_i}; \bar{Y} = \frac{\sum_{i=1}^n q_i \sin \theta_i}{\sum_{i=1}^n q_i} \quad (2)$$

250

251 Here, the equation (2) is derived using the weighted average of extreme events by weighing
252 the peak discharge. Here, \bar{X} and \bar{Y} represent the x- and y-coordinates of the mean event
253 date. Based on the time of occurrence of a flood event in a year, the mean event angle is
254 obtained by

$$Mean\ Angle = \begin{cases} \tan^{-1}\left(\frac{\bar{Y}}{\bar{X}}\right), & \text{if } \bar{X} > 0 \text{ and } \bar{Y} > 0 \\ 180 - \tan^{-1}\left(\frac{\bar{Y}}{\bar{X}}\right), & \text{if } \bar{X} < 0 \text{ and } \bar{Y} > 0 \\ 180 + \tan^{-1}\left(\frac{\bar{Y}}{\bar{X}}\right), & \text{if } \bar{X} < 0 \text{ and } \bar{Y} < 0 \\ 360 - \tan^{-1}\left(\frac{\bar{Y}}{\bar{X}}\right), & \text{if } \bar{X} > 0 \text{ and } \bar{Y} < 0 \end{cases} \quad (3)$$

255 The mean event date can then be determined as:

$$Mean\ Date = Mean\ Angle \times \left(\frac{len\ yr}{2\pi}\right) \quad (4)$$

256 Where *Mean Date* is the average date of occurrence of the extreme events. The persistence (

257 \bar{r}) of extreme events can be determined from:

258

$$\bar{r} = \sqrt{\bar{X}^2 + \bar{Y}^2}, \quad 0 \leq \bar{r} \leq 1 \quad (5)$$

259 The dimensionless ‘*r*’ indicates the variability in the timing of flood events with $\bar{r} = 0$,

260 indicates no persistence, i.e., flood events are uniformly distributed throughout the year,

261 whereas, $\bar{r} = 1$ indicates high persistence, i.e., all floods at a station occur on the same day

262 of the year (Laaha and Blöschl, 2006). Mean date of flood occurrence may occur at a period

263 of the year when no events are observed (Burn and Whitfield, 2018). Circular variance

264 provides the variability of peak discharge events about the mean date for individual stations

265 (Dhakal et al., 2015). The long-term evolution of the circular variance σ^2 is computed using

266 the circular variance.

$$\sigma^2 = -2\ln(\bar{r}) \quad (6)$$

267 The trend in the timing of floods was estimated by the nonparametric adjusted Theil-Sen
 268 slope estimator. The trend estimator β_{circular} is the median of the difference of dates over all
 269 possible pairs of years (i and j) within the time series,

270

$$\beta_{\text{circular}} = \text{median} \left(\frac{\text{Julian Date}_j - \text{Julian date}_i + k}{j - i} \right) \quad (7)$$

271

With

$$k = \begin{cases} -\bar{m} & \text{if } (\text{Julian Date}_j - \text{Julian date}_i) > \bar{m} / 2 \\ \bar{m} & \text{if } (\text{Julian Date}_j - \text{Julian date}_i) < -\bar{m} / 2 \\ 0, & \text{otherwise} \end{cases} \quad (8)$$

Where,

$$\bar{m} = \frac{1}{n} \sum_{i=1}^n (\text{len yr})_i \quad (9)$$

272

273 Where k adjusts to the circular nature of the dates and β has units of days per year.

274

275 **3. Results**

276 *3.1 Presence of Spatially Coherent Monotonic trends and Abrupt Change Points*

277 Presence of monotonic trends in flood time series at individual stream gauges is evaluated
 278 using the Mann-Kendall trend test with correction for ties and autocorrelation. Figure 3
 279 shows the spatial trends in Monsoon peak discharge (June to September) and POT discharge
 280 events for all the 24 gauge stations in MRB. While none of the monsoonal maxima discharge
 281 events showed a local significant increasing trend (at 10% significance level) using MMPD

282 time series (Fig. 3(a)), the POT discharge events showed significant increasing trends at
283 Kurubhata, Hirakud Dam and Kantamal gauging stations (Fig. 3(b)). In both MMPD and
284 POT flood trends, Region I exhibited a mixture of increasing and decreasing trends with the
285 latter dominating the former. This might be the consequence of changing rainfall patterns
286 over the basin and a significant decreasing rainfall trends over the basin, especially during
287 August (Panda et al., 2013). Further, since there is no major control structure upstream of the
288 Hirakud reservoir, the stream flow at most of the gauging sites upstream to Hirakud reservoir
289 can be considered unregulated (Panda et al., 2013).

290

291 Most of the stations in Region II except Tikarapara showed increasing trends (either
292 significant or insignificant). For example, despite the presence of dense deciduous vegetative
293 cover, an increasing trend in flood magnitude at Kantamal sub-basin could be attributed to
294 deforestation at the upstream sub-basins as reported in an earlier study (Mishra et al., 2008).
295 Also, the review of the literature (Jena et al., 2014) suggests, the recent (post-1957, the year
296 of Hirakud dam construction) incidence of high floods in this region is due to an increase in
297 extreme rainfall in the middle reaches of the basin. An insignificant decreasing trend at
298 Tikarapara gauge station is due to the dense vegetative cover, and the medium textured soil
299 type over the watershed area, which amplifies the infiltration processes and hence reducing
300 runoff over the basin (CWC, 2014). An insignificant increasing trend at Naraj gauge station
301 could be attributed to proximity to the coast of the Bay of Bengal and high-tide induced
302 flooding across the delta (distance between Naraj gauging station and the coastline of the Bay
303 of Bengal is only 120 km) region that could extend inwards due to small width of the delta

304 (Choudhury et al., 2012). As extreme sea level resulting from severe storm surges across the
305 Bay of Bengal (Flierl and Robinson, 1972; Milliman et al., 1989) pushes ocean tides
306 upstream, the tidal signal propagates from river estuaries to inland, which in turn can amplify
307 the risk of flooding in delta region (Ensign and Noe, 2018; Lyddon et al., 2018). The floods
308 in the low-lying delta region can stem from the superposition of storm surges and river floods,
309 which is frequently associated with common meteorological drivers, such as low-pressure
310 synoptic systems and extreme precipitation. The moisture-laden air-mass from coast move
311 inland over the catchment leading to heavy and persistent rainfall, causing inland flooding.
312 Our findings corroborate well with Panda et al. (2013), in which the authors identified
313 significant upward trends in rainfall across the southwestern and coastal parts of the basin.
314 The synoptic disturbances over the Bay of Bengal, leading to flash flood generating extreme
315 rainfalls (Panda et al., 2013) could be the potential causes of increasing flood trends in this
316 region. Then we apply a field significance test to understand regional behavior of trend across
317 MRB, which indicated a downward trend (significant) over Region I for MMPD events at
318 10% significance level. On the other hand, the middle region does not show any field
319 significant upward or downward trend. Further, we could not find the presence of any
320 significant trend for the POT time series across the regions. Table S2 presents the results of
321 field significance test in all regions across MRB.

322

323 Next, we detect abrupt changes in the flood time series using the Pettitt test. Change points
324 in a long historical data arises due to multiple consequences such as a shift in gauge location,
325 changes in land use and land cover, reservoir regulations, as well as climatic variations

326 (Villarini et al., 2009a). Fig. 4 shows the identification of change points (in location or mean
327 of the distribution) of MMPD and POT events.

328

329 In MMPD events (Fig. 4(a)), only 3 (16.67% of all the stations over MRB) out of 24 stations
330 in the basin show statistically significant change points at 10% significance level. The stream
331 gauge location, Andhiyarkore shows a presence of significant change point at 15%
332 significance level. For POT events (Fig. 4(b)), two stations (Bamnidhi and Manendragarh)
333 exhibits abrupt changes at 10% significance level while Kurubhata gauge station shows
334 significant change point at 15% significance level. None of the stations had a change point
335 at 5% significance level.

336

337 A closer look reveals, all these stations are spatially distributed over the northern part of the
338 basin at Region I. It was observed that all these stations (i.e., Andhiyarkore, Bamnidhi,
339 Ghatora, Kurubhata, and Manendragarh) had a change point during the end of the 20th and
340 beginning of the 21st centuries. However, it should be noted that no discernible spatial
341 patterns could be identified based on the detected change points with respect to the mean.
342 Further, the detected change points at Bamnidhi (1987 and 1978 for MMPD and POT events,
343 respectively) and Manendragarh (2003 and 2004 for MMPD and POT events, respectively)
344 are close to the year of construction of ‘mega-dams’ (1985, 1976 and 2004) with a height >
345 15 m (Best, 2019) up-streams to the respective gauge stations (WRIS, 2015). Details of these
346 dams, their capacity, and the corresponding gauge locations are presented in Table S3. For
347 remaining stream gauges, we could not identify any specific reasons for the abrupt changes.

348

349 To summarize, our findings suggest following in relation to flood trends across MRB: (i) for
350 MMPD events, ~ 67% (12 out of 18 stations) gauge stations showed (either significant or
351 insignificant) decreasing trend in flood magnitude at Region I, whereas 67% (4 out of 6
352 stations) gauge stations showed (insignificant) increasing trend across Region II. (ii) For POT
353 events, at region I, ~ 56% (10 out of 18 stations) gauge stations showed spatially coherent
354 (either significant or insignificant) decreasing trends, whereas, at Region II, 80% (4 out of 5
355 stations) gauge stations showed (either significant or insignificant) increasing trends in flood
356 magnitude. (iii) Overall, a larger number of stations show upward trends in flood magnitude
357 for POT events (52% stations) than that of the MMPD event (42% stations) (iv) On the other
358 hand, ~ 17% and 13% of the stations show change points for MMPD and POT events,
359 respectively.

360

361 *3.2 Little Evidence of Scale-Dependency in the Nature of Flood Samplings*

362 Next, we analyze the influence of scale-dependency in the results of trend estimates. The
363 objective of the scale-dependency test is to investigate if the nature of changes in streamflow
364 patterns is related to the catchment size and elevation of the basins. For this, the relative
365 changes in each of the flood indicators are plotted against the basin area and mean basin
366 elevation. Fig. 5 presents three-dimensional plots to analyze the role of catchment size and
367 mean basin elevation on flood trends. The significant changes are marked (Fig. 5) in solid.
368 We observe no clear pattern of scale-dependency across MRB. There are no spatial scales
369 and elevations, where significant changes are concentrated. However, for MMPD events,

370 decreasing trends are more concentrated between 1000 and 3000 km² catchment area and the
371 mean elevation between 490 and 700 m MSL (Fig. S1). However, none of these downward
372 trends are statistically significant. On the other hand, a few evidence of significant increasing
373 trends (at three of the gauging stations, Kurubhata, Kantamal, and Hirakud dam) are observed
374 for larger catchments (catchment area more than 1000 km²) with higher basin elevation
375 (ranges between 250 and 500 m MSL) for the POT flood events (Fig. S1). Despite locating
376 at a higher elevation, the downward trend in Manendragarh station for both flood series is
377 attributed to the construction of mega-dams upstream in 2004 (Table S3).

378

379 *3.3 No Notable Changes in Flood Seasonality*

380 The seasonality in flood responses is determined using directional statistics. The changes in
381 the timing (mean date), flood variability (σ) and persistence (\bar{r}) are evaluated for individual
382 stream gauge locations. Seasonality measures of MMPD and POT peak discharge events are
383 plotted in a polar plot as shown in Fig. 6. The mean occurrence date of flood for each of the
384 station is represented as an angle measured counterclockwise relative to 1st January, and the
385 persistence of the flood events are shown as the distance from the center of the polar plot.
386 The circular variance (σ^2) for individual gauge stations are represented by the size of
387 respective circles, with small circle size indicating less variance and large circle size
388 indicating more variance. Fig. 7 gives information on the mean date of flood events in details.
389 The x-axis represents the mean date of MMPD and POT peak discharge events in the August
390 month.

391

392 For both MMPD and POT peak discharge events, the seasonality analysis indicates the
393 persistence of floods across all gauges with mean flood dates occurring in August. For
394 majority of the gauging station, the mean flood dates are concentrated around the second
395 week of August for both MMPD and POT events with the exception for Andhiarkore gauge
396 station, situated at the Upper MRB (Region I), which showed the mean flood date close to
397 September (28 August) for the MMPD events (Fig. 6 (a)). However, considering both
398 methods for flood samplings, the POT events show relatively less regular mean flood dates
399 with higher circular variance than that of the MMPD events. Taken together, we infer that
400 the peak discharge events are highly regular in MRB. Our results are in agreement with Burn
401 and Whitfield (2018), in which authors found that stream gauges in the pluvial flood regime,
402 in general, show a very few (significant) changes in flood seasonality than that of the other
403 flood regimes.

404

405 *3.4 Shifts in the timing of flood peaks*

406 The shifts in the timing of flood peaks are analyzed using an adjusted Theil - Sen slope
407 estimator with the correction for the circular nature of mean dates. Fig. 8 summarizes the
408 results of changes in timings of MMPD and POT discharge events in MRB. While the
409 location of the stream gauges is represented using a square box, the hues in red and green of
410 the boxes indicate the gauges with earlier and late occurrences of peak discharge events. The
411 stream gauge with color in white represents the flood events that have concurred with the
412 mean flood date at respective stream gauge location, whereas darker shades show a
413 substantial deviation from the mean flood date. For POT series, we exclude Naraj station

414 from the analysis (Fig. 8(b)) since the number of discharge events was found to be less than
415 ten for this site.

416

417 For the MMPD events (Fig. 8(a)), most of the stations in Region II showed an earlier
418 occurrence of peak discharge events. At Delta region, Naraj located at relatively low
419 elevation (Table S1) shows a delay in flood occurrence up to 18 days (per decade). While the
420 stream gauge at Manendragarh, situated at a relatively higher elevation (Table S1),
421 experiences an earlier appearance of flood date. In contrast to MMPD events, for POT events
422 (Fig. 8(b)), we find no shifts in flood timings across most of the gauges at region II, rather
423 surprisingly a delayed occurrence of peak event at Kesinga. A few gauging stations show
424 disparate trends in flood timing for MMPD and POT events, with an earlier occurrence of
425 flood for MMPD events while delayed for the POT event and vice versa.

426

427 For both methods of flood samplings, the Hirakud dam showed a delayed date of flood
428 occurrence, whereas, Tikarpara near the delta showed an earlier appearance of floods. The
429 delay in flood dates in Hirakud could be attributed to a shift towards greater water inflow
430 during September in Hirakud reservoir in recent decades as shown in a latest report
431 (Choudhury et al., 2012) based on analysis of trends of mean inflow (1958-2008) records.
432 The delayed flood timing in Hirakud has critical implications for flood control operation of
433 the dam since, by the monsoon end (i.e., during September), dam management authorities
434 are in a dilemma whether to open the reservoir gate. For instance, severe floods in
435 downstream of Hirakud during the year 2001, 2008 and 2011 (Brakenridge, 2018; Jena *et al.*,

436 2014) were triggered by the delay in releasing water from several full dams coupled with
437 abnormally heavy monsoonal precipitation. On the other hand, an earlier flood occurrence at
438 Tikarpara could be attributed to the loss of forest cover area across the middle reaches of the
439 basin (Dadhwal et al., 2010). Based on modeling of streamflow across the Mahanadi basin
440 (with an outlet at Munduli, which is located at 4.5 km upstream to Naraj), Dadhwal *et al.*
441 (2010) concluded that the decrease in forest cover by about 5.7% have resulted in an increase
442 in fluvial discharge by approximately 4.5% at Munduli in the delta. Furthermore, the heavy
443 rainfall induces a massive inflow in the Hirakud reservoir leading to the dam authorities to
444 open gates of the dam, causing flash floods in the delta region (Panda et al., 2013).

445

446 For region I, ~56% (10 out of 18) and 61% (11 out of 18) of the stations show delay in flood
447 occurrences for both MMPD events and POT events respectively, while at region II, ~ 67%
448 (4 out of 6) exhibits earlier dates of floods for MMPD events, whereas, no shifts in flood
449 timing is observed for POT events at 60% (3 out of 5) stations. Overall, our results suggest
450 more number of stream gauges show delayed flood occurrence for both methods of flood
451 samples.

452

453 It is interesting to note that for both methods of flood samplings, we find sites with upward
454 (downward) trends in flood magnitude, however, with delayed (earlier) dates of flood
455 occurrences. Considering basin as a whole, ~33% and ~17% of the stations unveiled a
456 downward trend in flood magnitude with an earlier date of flood occurrence for MMPD and
457 POT events respectively. On the other hand, ~29% - 35% of the stations show upward trends

458 in flood magnitude with a delayed shift in flood timings for both methods of flood samplings.
459 Table S4 presents the list of these stations name.

460

461 **4. Discussion and conclusions**

462 This paper contributes to the comprehensive assessment of flood trends in densely populated
463 Mahanadi river basin. Unlike previous assessments (Jena et al., 2014; Panda et al., 2013),
464 here we investigate three novel aspects: *first*, a comparative analysis of spatial patterns in
465 (either significant or insignificant) upward/downward trends in two different flood series
466 derived from the monsoonal maximum (MMPD) and peak over threshold (POT) events.
467 While monotonic trends in flood series are evaluated using nonparametric Mann Kendall
468 trend statistics, the abrupt shifts in flood time series are detected using Pettitt test for single
469 change-point analysis. Besides, assessing the results of local significance at individual stream
470 gauge locations, we evaluated the regional trend using field significance test. Second, we
471 assess the sensitivity of flood magnitudes trends concerning catchment size and mean basin
472 elevation. Finally, we assess the persistence of the flood events and shifts in the timing of
473 flood flow using directional statistics. While most of the earlier assessments are limited to
474 the river basins across mid- and high latitude nations, to the best of our knowledge, this study
475 is the first to assess the seasonality and shift in the date of flood occurrences in a large tropical
476 river basin, MRB (MRB as a whole consist of a drainage area of 1,41,589 km², the mean
477 annual discharge is 1,895 m³/s with a maximum of 6,352 m³/s during monsoon months
478 [Dadhwal et al., 2010]). By leveraging in-situ observations, our analyses detect flood rich
479 and flood poor region across MRB, which can serve as a basis for attributing hydrologic

480 response to climate change under the effect of multiple drivers (Vano et al., 2015; Vano and
481 Lettenmaier, 2014).

482

483 Although detected trends in flood magnitude (Fig. 1) and shifts (delayed or earlier) in timing
484 of floods (Fig. 8; Table S4) over MRB could be linked to human intervention (Best, 2019;
485 Choudhury et al., 2012; Dadhwal et al., 2010; Mishra et al., 2008) rainfall-induced runoff
486 during monsoon season (June – September) is one of the major flood generating drivers in
487 the basin (Jena et al., 2014; Panda et al., 2013). Further, upward trends in floods in the delta
488 region could be attributed to superposition of extreme sea level, such as severe storm surges
489 (Flierl and Robinson, 1972; Milliman et al., 1989) and river floods in the delta region, which
490 is frequently associated with a severe storm resulting from synoptic low-pressure systems
491 and extreme precipitation. One of the plausible physical mechanisms is to link extreme
492 precipitation event to an increase in the magnitude of river floods in a warming climate.
493 Despite most of the gauges in the middle reaches show an upward trend in flood magnitude,
494 our analyses based on the seasonality index indicate a relatively regular peak discharge
495 (persistence index ranges between 0.88 and 0.95 for MMPD events and 0.87 and 0.92 for
496 POT events) with mean date of flood occurrences during the mid of August for most of the
497 gauges. These results indicate that flood events are mostly modulated by changes in flood
498 generating processes (available antecedent moisture content in the catchment and shift in
499 atmospheric circulation pattern that results into change in dominant storm mechanism) rather
500 than the increase in precipitation extremes in response to increase in surface warming
501 (Sharma et al., 2018; Wasko and Sharma, 2017). The review of the literature suggests

502 (Pattanayak et al., 2017) a linkage between large-scale atmospheric circulation pattern (such
503 as sea surface temperature, SST) and basin hydroclimatology (such as precipitation,
504 temperature minima, and temperature maxima) over MRB. A strong linkage was identified
505 especially during the 1980s, which was attributed to changes in Pacific Decadal SST patterns
506 and anthropogenic effects (Pattanayak et al., 2017).

507

508 The key insights from the study are summarized as follows:

509 • A spatially coherent pattern of the flood is observed in MRB using both methods of
510 flood samplings - Region I shows a mixture of (insignificant) increasing and decreasing
511 trend, in which the number of gauges with downward trends is more than that of the
512 number gauges with upward trends. While the majority of gauges show evidence of
513 insignificant up/downward trends in flood magnitude (at 10% significance level), only
514 Bamnidhi and Manendragarh show (significant) downward trends, whereas Kurubhata
515 shows a (significant) upward trend in flood magnitude. On the other hand, at Region
516 II, the middle reach of MRB, we find most of the stations show (either
517 significant/insignificant) upward trends. Further, the downward trends in Region I are
518 field significant. Also, while we find a few evidences of (significant) change points at
519 Region I, no such change points are detected across the Region II.

520

521 • Except for construction of a few major dams upstream that have affected the nature of
522 flood trends, overall, we observe no clear linkage between flood severity and catchment
523 morphology (i.e., mean basin elevation and watershed area). For MMPD events

524 (insignificant) downward trends in flood magnitude for stream gauges (out of which
525 two of them is statistically significant) are clustered between 1000 and 3000 km² area
526 with elevation ranges from 490 – 700 m MSL. On the other hand, for POT event, we
527 find a few evidence of a significant upward trend for larger catchment (of an area more
528 than 1000 km²) with high basin elevation (between 250 and 500 m MSL). The stream
529 gauge at Manendragarh, located at upstream gauges of MRB showed a downward trend
530 in flood magnitude for both MMPD as well POT events despite being located at higher
531 elevation (668m above mean sea level) and smaller catchment area (~ 1000 km²), which
532 is attributed to construction of a dam near this site.

533

534 • The seasonality of flood responses in both methods of flood samplings suggests the
535 mean date of flood occurrences are concentrated around the mid of August for most of
536 the stream gauges with the exception for the Andhiarkore at Region I, for which the
537 mean flood date is closed to September (28th August) for MMPD events. Although we
538 note the nature of mean date of flood occurrences are more or less uniform across both
539 methods of flood samplings, the POT events show relatively less regular mean flood
540 dates with higher circular variance than that of the MMPD events.

541

542 • Around half of the stream gauges across MRB exhibit delay in the date of flood
543 occurrences, which is in agreement with both methods of flood samplings. About ~29%
544 (~33%) and ~35% (~17%) of the stations indicate an upward (downward) trend but
545 with delay (early) occurrence of floods for MMPD and POT events, respectively.

546

547 Although we find a spatially coherent flood pattern in MRB using both methods of flood
548 samplings, the nature of trends differs case by case basis. This is because, while in monsoonal
549 maxima event, we select the maximum peak flow of each year during monsoon month (June
550 to September), POT sample are extracted from all peak values from the total time series that
551 lie above a certain truncation level, while ensuring each of the selected samples are
552 independent of one another. Thus, a very low discharge value, especially during a dry period,
553 can also be a part of MMPD event, whereas, some peaks that are not MMPD but are still very
554 high could be a part of POT event (Bezak et al., 2014).

555

556 A few caveats could be considered. We considered trends in flood magnitudes and
557 seasonality in flood occurrences across MRB using ground-based observation. The specific
558 insights are conditioned on the quality of site-specific information used in the analyses. Based
559 on the availability of good quality in-situ observations, the analysis is limited to the recent
560 four decades. Although many studies so far analyzed the influence of hydro-meteorological
561 drivers, precipitation and air temperature in generating peak discharge across MRB, no
562 studies, to date analyzed the role of catchment wetness in simulating the nature of floods.
563 However, extreme precipitation does not necessarily lead to fluvial floods (Sharma et al.,
564 2018; Wasko and Sharma, 2017), antecedent catchment wetness often strongly controls the
565 nature of flood peaks across the river basin (Merz et al., 2018; Schröter et al., 2015). Hence,
566 future research will be directed towards understanding the role of catchment processes, such

567 as antecedent moisture content, in modulating the nature of flood flows in a large river basin
568 system, such as in MRB.

569

570 **Acknowledgments**

571 The authors sincerely thank the Department of Science and Technology (DST), Government
572 of India, for the financial support. This study was organized as a part of the Center of
573 Excellence (CoE) in Climate Change studies activity established at IIT Kharagpur and funded
574 by DST, Government of India. This study forms a part of the sub-project “Impact of Climate
575 Change on Flood Risk” conducted under the CoE in Climate Change at IIT Kharagpur. We
576 are also thankful to the Central Water Commission (CWC), Government of India, for
577 providing the data sets for this research.

578

579 **Author contribution**

580 The first author carried out the analyses under the guidance of the second and the third author
581 and prepared the first draft. The second author conceived the idea and helped in writing the
582 manuscript. All three authors interpreted the results, contributed in writing and reviewed the
583 manuscript.

584

585

586

587 **List of Figure Captions**

588 Fig. 1. Mahanadi river basin (a) Elevation map (b) District wise population density with
589 highlighting major cities (Census data 2011).

590 Fig.2. Flowchart summarizing the workflow.

591 Fig. 3. Spatial trends at the 10% significance level (a) MMPD events and (b) POT events.
592 The size of a triangle is proportional to the magnitude of trends calculated by the
593 Theil Sen slope estimator.

594 Fig. 4. Change point analysis (Pettitt test) of (a) MMPD events and (b) POT events for gauge
595 stations at a significance level of 5, 10 and 15%, respectively. While the single change
596 point analysis is performed by the Pettitt test, differences in mean stream flow after
597 and before the detected change points are shown using the triangle. The downward
598 orientation of the triangle indicates a decrease in mean stream flow after change point
599 years at respective gauge location.

600 Fig. 5. Scale dependency relative to flood trends of MMPD events (*upper panel*) and POT
601 events (*lower panel*). Mann-Kendall trend statistics are plotted as a function of the
602 Catchment size (in km²) and Catchment elevation (in m). Shaded triangles indicate
603 significant changes at the 10% significance level.

604 Fig. 6. The circular plots of mean date and persistence of floods using (*left panel*) MMPD
605 and (*right panel*) POT events. The size of the circle indicates the value of circular
606 variance with larger (smaller) size indicates a larger (smaller) variance.

607 Fig. 7. Mean occurrence dates of Monsoonal Peak Discharge (MMPD) and Peak over
608 Threshold (POT) flood events.

609 Fig. 8. Trends in flood timing of (a) MMPD events and (b) POT events at individual gauge
610 stations. The shift in the date of flood occurrences is calculated in days per decade.

611

612 **List of Table Caption**

613 **Table 1.** Summary of some past relevant studies and their key insights

614 **References**

- 615 Bawden, A.J., Linton, H.C., Burn, D.H., Prowse, T.D., 2014. A spatiotemporal analysis of
616 hydrological trends and variability in the Athabasca River region, Canada. *J. Hydrol.*
617 509, 333–342. <https://doi.org/10.1016/j.jhydrol.2013.11.051>.
- 618 Benjamini, Y., Hochberg, Y., 1995. Controlling the False Discovery Rate : A Practical and
619 Powerful Approach to Multiple Testing. *R. Stat. Soc.* 57, 289–300.
- 620 Benjamini, Y., Yekutieli, and D., 2001. The control of the false discovery rate in multiple
621 testing under dependency. *Ann. Stat.* 29, 1165–1188.
622 <https://doi.org/10.1214/aos/1013699998>.
- 623 Beura, D., 2015. Floods in Mahanadi river, Odisha, India: its causes and management. *Int. J.*
624 *Eng. Appl. Sci.* 2, 51–55.
- 625 Bezak, N., Brilly, M., Šraj, M., 2014. Comparaison entre les méthodes de dépassement de
626 seuil et du maximum annuel pour les analyses de fréquence des crues. *Hydrol. Sci. J.*
627 59, 959–977. <https://doi.org/10.1080/02626667.2013.831174>.
- 628 Best, J., 2019. Anthropogenic stresses on the world’s big rivers. *Nature Geoscience.* 12, 7-
629 21.
- 630 Blöschl, G., Hall, J., Parajka, J., Perdigão, R.A.P., Merz, B., Arheimer, B., Aronica, G.T.,
631 Bilibashi, A., Bonacci, O., Borga, M., Čanjevac, I., Castellarin, A., Chirico, G.B., Claps,
632 P., Fiala, K., Frolova, N., Gorbachova, L., Gül, A., Hannaford, J., Harrigan, S., Kireeva,
633 M., Kiss, A., Kjeldsen, T.R., Kohnová, S., Koskela, J.J., Ledvinka, O., Macdonald, N.,
634 Mavrova-Guirguinova, M., Mediero, L., Merz, R., Molnar, P., Montanari, A., Murphy,
635 C., Osuch, M., Ovcharuk, V., Radevski, I., Rogger, M., Salinas, J.L., Sauquet, E., Šraj,
636 M., Szolgay, J., Viglione, A., Volpi, E., Wilson, D., Zaimi, K., Živković, N., 2017.
637 Changing climate shifts timing of European floods. *Science (80-.).* 357, 588–590.
638 <https://doi.org/10.1126/science.aan2506>.
- 639 Brakenridge, G.R., 2018. Global Active Archive of Large Flood Events. Available at:
640 <http://floodobservatory.colorado.edu/>. [Accessed 21 August 2018].
- 641 Burn, D.H., Sharif, M., Zhang, K., 2010. Detection of trends in hydrological extremes for
642 Canadian watersheds. *Hydrol. Process.* 24, 1781–1790.
643 <https://doi.org/10.1002/hyp.7625>.

- 644 Burn, D.H., Whitfield, P.H., 2018. Changes in flood events inferred from centennial length
645 streamflow data records. *Adv. Water Resour.* 121, 333–349.
646 <https://doi.org/10.1016/j.advwatres.2018.08.017>.
- 647 Burn, D.H., Whitfield, P.H., Sharif, M., 2016. Identification of changes in floods and flood
648 regimes in Canada using a peaks over threshold approach. *Hydrol. Process.* 30, 3303–
649 3314. <https://doi.org/10.1002/hyp.10861>.
- 650 CWC (Central Water Commission), 2014. Mahanadi Basin (No. Version 2). CWC and
651 NRSC, New Delhi.
- 652 Chandra, S., 2018. State wise flood damage statistics. CWC, Government of India.
- 653 Choudhury, P., Sandbhor, J., Satapathy, P., 2012. Floods , Fields and Factories : Towards
654 Resolving Conflicts around the Hirakud Dam Forum for Policy Dialogue on Water
655 Conflicts in India.
- 656 Cunderlik, J.M., Ouarda, T.B.M.J., 2009. Trends in the timing and magnitude of floods in
657 Canada. *J. Hydrol.* 375, 471–480. <https://doi.org/10.1016/j.jhydrol.2009.06.050>.
- 658 Cunderlik, J.M., Ouarda, T.B.M.J., Bobée B. 2004. Determination of flood seasonality from
659 hydrological records. *Hydrol. Sci. J.* 49 (3), 511–526.
- 660 Dadhwal, V.K., Mishra, N., Aggarwal, S, P., 2010. Hydrological Simulation of Mahanadi
661 River Basin and Impact of Land Use / Land Cover Change on Surface Runoff Using a
662 Macro Scale Hydrological Model. ISPRS TC VII Symp. – 100 Years ISPRS, Vienna,
663 Austria XXXVIII, 165–170.
- 664 Dhakal, N., Jain, S., Gray, A., Dandy, M., Stancioff, E., 2015. Nonstationarity in seasonality
665 of extreme precipitation: A nonparametric circular statistical approach and its
666 application. *Water Resour. Res.* 51, 4499–4515.
667 <https://doi.org/10.1002/2014WR016399>.
- 668 Ensign, S.H., Noe, G.B., 2018. Tidal extension and sea-level rise: recommendations for a
669 research agenda. *Front. Ecol. Environ.* 16, 37–43. <https://doi.org/10.1002/fee.1745>.
- 670 Fisher, N.I., Lewis, T., Embleton B.J.J., 1993. Statistical analysis of spherical data.
671 Cambridge university press.

- 672 Flierl, G.R., Robinson, A.R., 1972. Deadly Surges in the Bay of Bengal: Dynamics and
673 Storm-tide Tables. *Nature* 239, 213–215. <https://doi.org/10.1038/239213a0>.
- 674 Halgamuge, M.N., Nirmalathas, A., 2017. Analysis of large flood events: Based on flood
675 data during 1985–2016 in Australia and India. *Int. J. disaster risk Reduct.* 24, 1–11.
- 676 Hall, J., Arheimer, B., Borga, M., Brázdil, R., Claps, P., Kiss, A., Kjeldsen, T.R.,
677 Kriaučiuniene, J., Kundzewicz, Z.W., Lang, M., Llasat, M.C., Macdonald, N., McIntyre,
678 N., Mediero, L., Merz, B., Merz, R., Molnar, P., Montanari, A., Neuhold, C., Parajka,
679 J., Perdigoão, R.A.P., Plavcová, L., Rogger, M., Salinas, J.L., Sauquet, E., Schär, C.,
680 Szolgay, J., Viglione, A., Blöschl, G., 2014. Understanding flood regime changes in
681 Europe: A state-of-the-art assessment. *Hydrol. Earth Syst. Sci.* 18, 2735–2772.
682 <https://doi.org/10.5194/hess-18-2735-2014>.
- 683 Hall, J., Solomatine, D., 2008. A framework for uncertainty analysis in flood risk
684 management decisions. *Int. J. River Basin Manag.* 6, 85–98.
685 <https://doi.org/10.1080/15715124.2008.9635339>.
- 686 Hamed, K.H., Ramachandra Rao, A., 1998. A modified Mann-Kendall trend test for
687 autocorrelated data. *J. Hydrol.* 204, 182–196. [https://doi.org/10.1016/S0022-1694\(97\)00125-X](https://doi.org/10.1016/S0022-1694(97)00125-X).
- 689 Hirabayashi, Y., Mahendran, R., Koirala, S., Konoshima, L., Yamazaki, D., Watanabe, S.,
690 Kim, H., Kanae, S., 2013. Global flood risk under climate change. *Nat. Clim. Chang.* 3,
691 816–821. <https://doi.org/10.1038/nclimate1911>.
- 692 Jarvis, A., H.I., Reuter, A., Nelson, A., Guevara, E., 2008. Hole-filled SRTM for the globe
693 Version 3, available from the CGIAR-CSI SRTM 90m Database. CGIAR CSI Consort.
694 *Spat. Inf.* 1–9. <https://doi.org/10.1167/iov.10-6319>.
- 695 Jena, P.P., Chatterjee, C., Pradhan, G., Mishra, A., 2014. Are recent frequent high floods in
696 Mahanadi basin in eastern India due to increase in extreme rainfalls? *J. Hydrol.* 517,
697 847–862. <https://doi.org/10.1016/j.jhydrol.2014.06.021>.
- 698 Kendall, M.G., 1975. *Rank Correlation Methods*. Charles Griffin: London.
- 699 Khaliq, M.N., Ouarda, T.B.M.J., Gachon, P., Sushama, L., St-Hilaire, A., 2009. Identification

- 700 of hydrological trends in the presence of serial and cross correlations: A review of
701 selected methods and their application to annual flow regimes of Canadian rivers. *J.*
702 *Hydrol.* 368, 117–130. <https://doi.org/10.1016/j.jhydrol.2009.01.035>.
- 703 Kunkel, K.E., Andsager, K., Easterling, D.R., 1999. Long-term trends in extreme
704 precipitation events over the conterminous United States and Canada. *J. Clim.* 12, 2515–
705 2527. [https://doi.org/http://dx.doi.org/10.1175/1520-
706 0442\(1999\)012<2515:LTTIEP>2.0.CO;2](https://doi.org/http://dx.doi.org/10.1175/1520-0442(1999)012<2515:LTTIEP>2.0.CO;2).
- 707 Kwon, H.H., Brown, C., Lall, U., 2008. Climate informed flood frequency analysis and
708 prediction in Montana using hierarchical Bayesian modeling. *Geophys. Res. Lett.* 35(5),
709 1-6. <https://doi.org/10.1029/2007GL032220>.
- 710 Laaha, G., Blöschl, G., 2006. Seasonality indices for regionalizing low flows. *Hydrol.*
711 *Process.* 20 (18), 3851–3878.
- 712 López, J., Francés, F., 2013. Non-stationary flood frequency analysis in continental Spanish
713 rivers, using climate and reservoir indices as external covariates. *Hydrol. Earth Syst.*
714 *Sci.* 17, 3189–3203.
- 715 Lyddon, C., Brown, J.M., Leonardi, N., Plater, A.J., 2018. Flood Hazard Assessment for a
716 Hyper-Tidal Estuary as a Function of Tide-Surge-Morphology Interaction. *Estuaries*
717 *and Coasts* 41, 1565–1586. <https://doi.org/10.1007/s12237-018-0384-9>.
- 718 Mardia, K. V., 1972. Probability and mathematical statistics: statistics of directional data.
719 Academic Press.
- 720 Matti, B., Dahlke, H.E., Dieppois, B., Lawler, D.M., Lyon, S.W., 2017. Flood seasonality
721 across Scandinavia—Evidence of a shifting hydrograph? *Hydrol. Process.* 31, 4354–
722 4370.
- 723 Merz, B., Dung, N.V., Apel, H., Gerlitz, L., Schröter, K., Steirou, E., Vorogushyn, S., 2018.
724 Spatial coherence of flood-rich and flood-poor periods across Germany. *J. Hydrol.* 559,
725 813–826. <https://doi.org/10.1016/j.jhydrol.2018.02.082>.
- 726 Milliman J D Broadus J M Gable, F., 1989. Environmental and economic implications of
727 rising sea level and subsiding deltas: the Nile and Bengal examples. *Ambio* 18, 340–345.

- 728 <https://doi.org/10.2307/1052379>.
- 729 Mirza, M.M.Q., 2003. Climate change and extreme weather events: can developing countries
730 adapt? *Clim. policy* 3, 233–248.
- 731 Mishra, N., Aggarwal, S.P., Dadhwal, V.K., 2008. Macroscale Hydrological Modelling and
732 Impact of landcover change on streamflows of the Mahanadi River Basin. Master thesis,
733 Andhra University, Indian Institute of Remote Sensing (National Remote Sensing
734 Agency) Dept. of Space, Govt. of India 122.
- 735 Mondal, A., Mujumdar, P.P., 2012. On the basin-scale detection and attribution of human-
736 induced climate change in monsoon precipitation and streamflow. *Water Resour. Res.*
737 48, 1–18. <https://doi.org/10.1029/2011WR011468>.
- 738 Murray, V., Ebi, K.L., 2012. IPCC Special Report on Managing the Risks of Extreme Events
739 and Disasters to Advance Climate Change Adaptation (SREX). *J. Epidemiol.*
740 *Community Health* 66, 759–60. <https://doi.org/10.1136/jech-2012-201045>.
- 741 NIH (National Institute of Hydrology). 2018. Mahanadi Basin. Available at:
742 <http://nihroorkee.gov.in/rbis/>. [Accessed 16 August 2018].
- 743 Nka, B.N., Oudin, L., Karambiri, H., Paturel, J.E., Ribstein, P., 2015. Trends in floods in
744 West Africa: analysis based on 11 catchments in the region. *Hydrol. Earth Syst. Sci.* 19,
745 4707–4719. <https://doi.org/https://doi.org/10.5194/hess-19-4707-2015>.
- 746 Panda, D.K., Kumar, A., Ghosh, S., Mohanty, R.K., 2013. Streamflow trends in the mahanadi
747 river basin (India): Linkages to tropical climate variability. *J. Hydrol.* 495, 135–149.
748 <https://doi.org/10.1016/j.jhydrol.2013.04.054>.
- 749 Pattanayak, S., Nanjundiah, R.S., Kumar, D.N., 2017. Linkage between global sea surface
750 temperature and hydroclimatology of a major river basin of India before and after 1980.
751 *Environ. Res. Lett.* 12. <https://doi.org/10.1088/1748-9326/aa9664>.
- 752 Perreault, L., Bernier, J., Bobée, B., Parent, E., 2000. Bayesian change-point analysis in
753 hydrometeorological time series. Part 2. Comparison of change-point models and
754 forecasting. *J. Hydrol.* 235, 242–263. [https://doi.org/10.1016/S0022-1694\(00\)00271-7](https://doi.org/10.1016/S0022-1694(00)00271-7).
- 755 Petrow, T., Merz, B., 2009. Trends in flood magnitude, frequency and seasonality in

- 756 Germany in the period 1951-2002. *J. Hydrol.* 371, 129–141.
757 <https://doi.org/10.1016/j.jhydrol.2009.03.024>.
- 758 Pettitt, A. N., 1979. A Non-Parametric Approach to the Change-Point Problem. *J. R. Stat.*
759 *Soc. Ser. C (Applied Stat.)* 28, 126–135.
- 760 Pewsey, A., Neuhäuser, M., Ruxton, G.D., 2013. *Circular Statistics in R*. Oxford University
761 Press.
- 762 Reddy, M.J., Ganguli, P., 2013. Spatio-temporal analysis and derivation of copula-based
763 intensity-area-frequency curves for droughts in western Rajasthan (India). *Stoch.*
764 *Environ. Res. Risk Assess.* 27, 1975–1989. <https://doi.org/10.1007/s00477-013-0732-z>.
- 765 Regonda, S.K., Rajagopalan, B., Clark, M., Pitlick, J., 2005. Seasonal cycle shifts in
766 hydroclimatology over the western United States. *J. Clim.* 18, 372–384.
767 <https://doi.org/10.1175/JCLI-3272.1>.
- 768 Rodionov, S., 2005. A Brief Overview of the Regime Shift Detection Methods. *Large-Scale*
769 *Disturbances (Regime Shifts) Recover. Aquat. Syst. Challenges Manag. Towar. Sustain.*
770 17–24.
- 771 Rosner, A., Vogel, R.M., Kirshen, P.H., 2014. A risk-based approach to flood management
772 decisions in a nonstationary world. *Water Resour. Res.* 50, 1928–1942.
- 773 Schröter, K., Kunz, M., Elmer, F., Mühr, B., Merz, B., 2015. What made the June 2013 flood
774 in Germany an exceptional event? A hydro-meteorological evaluation. *Hydrol. Earth*
775 *Syst. Sci.* 19, 309–327. <https://doi.org/10.5194/hess-19-309-2015>.
- 776 Sharma, A., Wasko, C., Lettenmaier, D.P., 2018. If Precipitation Extremes Are Increasing,
777 Why Aren't Floods? *Water Resour. Res.* 8545–8551.
778 <https://doi.org/10.1029/2018WR023749>.
- 779 Stocker, T., n.d. *Climate change 2013: the physical science basis: Working Group I*
780 *contribution to the Fifth assessment report of the Intergovernmental Panel on Climate*
781 *Change*.
- 782 Storch, H. Von, Geesthacht, H., Navarra, A., 1999. *Analysis of Climate Variability* 10–26.
783 <https://doi.org/10.1007/978-3-662-03744-7>.

- 784 Svensson, C., Kundzewicz, Z.W., Maurer, T., 2005. Trend detection in river flow series: 2.
785 Flood and low-flow index series. *Hydrol. Sci. J.* 50, 811–824.
786 <https://doi.org/10.1623/hysj.2005.50.5.811>.
- 787 Tessler, Z.D., Vörösmarty, C.J., Grossberg, M., Gladkova, I., Aizenman, H., Syvitski, J.P.M.,
788 Fofoula-Georgiou, E., 2015. Profiling risk and sustainability in coastal deltas of the
789 world. *Science*. 349, 638–643. <https://doi.org/10.1126/science.aab3574>.
- 790 Thiel, H., 1950. A rank-invariant method of linear and polynomial regression analysis, Part
791 1. *Proceedings of the royal Netherlands academy of arts and science*. 53, 386–392.
- 792 Tian, P., Zhao, G., Li, J., Tian, K., 2011. Extreme value analysis of streamflow time series in
793 Poyang Lake Basin, China. *Water Sci. Eng.* 4, 121–132.
794 <https://doi.org/10.3882/j.issn.1674-2370.2011.02.001>.
- 795 Vano, J.A., Lettenmaier, D.P., 2014. A sensitivity-based approach to evaluating future
796 changes in Colorado River discharge. *Clim. Change* 122, 621–634.
797 <https://doi.org/10.1007/s10584-013-1023-x>.
- 798 Vano, J.A., Nijssen, B., Lettenmaier, D.P., 2015. Seasonal hydrologic responses to climate
799 change in the Pacific Northwest. *Water Resour. Res.* 51, 1959–1976.
800 <https://doi.org/10.1002/2014WR015909>.
- 801 Villarini, G., Serinaldi, F., Smith, J.A., Krajewski, W.F., 2009a. On the stationarity of annual
802 flood peaks in the continental United States during the 20th century. *Water Resour. Res.*
803 45, 1–17. <https://doi.org/10.1029/2008WR007645>.
- 804 Villarini, G., Smith, J.A., Serinaldi, F., Bales, J., Bates, P.D., Krajewski, W.F., 2009b. Flood
805 frequency analysis for nonstationary annual peak records in an urban drainage basin.
806 *Adv. Water Resour.* 32, 1255–1266. <https://doi.org/10.1016/j.advwatres.2009.05.003>.
- 807 Villarini, G., Smith, J.A., Serinaldi, F., Ntelekos, A.A., Schwarz, U., 2012. Analyses of
808 extreme flooding in Austria over the period 1951-2006. *Int. J. Climatol.* 32, 1178–1192.
809 <https://doi.org/10.1002/joc.2331>.
- 810 Vogel, R.M., Yaindl, C., Walter, M., 2011. Nonstationarity: flood magnification and
811 recurrence reduction factors in the United States1. *J. Am. Water Resour. Assoc.* 47,

812 464–474.

813 Wasko, C., Sharma, A., 2017. Global assessment of flood and storm extremes with increased
814 temperatures. *Sci. Rep.* 7, 1–8. <https://doi.org/10.1038/s41598-017-08481-1>.

815 WRIS (Water Resources Information System), India., 2015. Dams in Mahanadi Basin. Web
816 document. NRSC ISRO, Jodhpur. Available at: [http://india-
817 wris.nrsc.gov.in/wrpinfo/index.php?title=Dams_in_Mahanadi_Basin](http://india-wris.nrsc.gov.in/wrpinfo/index.php?title=Dams_in_Mahanadi_Basin), Accessed on:
818 February 2019.

Table 1. Summary of some past relevant studies and their key insights

Study	Region	Approach & Dataset Information	Key findings
<i>Petrow and Merz (2009)</i>	Throughout Germany	(i) Sites: 145 discharge gauges across Germany (ii) Period of analyses: 52 years (1951–2002) (iii) Data: Annual maximum series and peak over threshold discharge series (iv) Approach: Non-parametric Mann–Kendall test for trends in flood magnitude and frequency	(1) Most of the stations showed significant increasing flood trend (at 10% significance level). (2) Very few stations exhibited decreasing trends and were not field-significant. (3) Stations with significant trends were spatially clustered over the region.
<i>Tian et al. (2011)</i>	Poyang Lake Basin, China	(i) Sites: 10 hydrological stations were considered across Poyang Lake Basin (ii) Period of analyses: nearly 50 years of observed records (1957–2003) (iii) Data: Annual maximum and minimum flow, annual peak-over-threshold flows (iv) Approach: Non-parametric Mann-Kendall (MK) test and the linear regression method	(1) Both methods showed good agreement with each other in detecting flood trends. (2) Most annual maximum flows occurred between April to July, owing to southeast monsoon. (3) No significant upward/downward trends in flood magnitude are noted. (4) In contrast, a significant increasing trend was observed for low flow events.
<i>Panda et al. (2013)</i>	Mahanadi River Basin, India	(i) Sites: 19 gauging stations spread across the basin (ii) Period of analyses: 1972–2007 (iii) Data: Seasonal and sub-seasonal streamflow and rainfall variables were analyzed (iv) Approach: The Mann–Kendall nonparametric test after removing the serial correlation	(1) The streamflow was primarily controlled by the rainfall over the basin. (2) Increasing trends in flood magnitude in June while decreasing trends in August (3) Increased trends in both pre- and post-monsoon season streamflow and rainfall time series.

Trend analysis

<i>Bawden et al. (2014)</i>	Athabasca River Basin, Canada	<p>(i) Sites: 19 gauge stations of Athabasca River Basin</p> <p>(ii) Period of analyses: Varying record length between 1952 and 2010</p> <p>(iii) Data: Twenty flood indicators like annual and monthly mean flows, mean flow for the warm season, annual maximum and minimum daily flow were used</p> <p>(iv) Approach: Trend detection using the Mann–Kendall (MK) non-parametric test</p>	<p>(1) Strong decreasing trends in the annual warm season (March – October) and summer stream flows</p> <p>(2) Trends in streamflow were more strongly linked to precipitation than to air temperature</p>
<i>Jena et al. (2014)</i>	Mahanadi River Basin, India	<p>(i) Sites: Two gauge stations at upper and middle reaches of the basin</p> <p>(ii) Period of analyses: 1957-2011 for streamflow record and 1957-2007 for rainfall data</p> <p>(iii) Data: Annual peak streamflow releases and 1°×1° Gridded daily rainfall data.</p> <p>(iv) Approach: A non-parametric Mann–Kendall test</p>	<p>(1) The upper region of the basin showed no (significant) trend in rainfall while the middle region showed an increasing trend in rainfall.</p> <p>(2) The middle reach showed a significant increasing trend due to an upward trend in extreme rainfall in the middle reaches of the basin.</p>
<i>Bloschl et al. (2017)</i>	Entire Europe	<p>(i) Sites: 4262 hydrometric stations from 38 European countries</p> <p>(ii) Period of analyses: 1960-2010</p> <p>(iii) Data: Dates of occurrence of annual flood peaks</p> <p>(iv) Approach: Circular statistics, Theil-Sen slope estimator and a centered 10-year moving average method</p>	<p>(1) Earlier spring snowmelt floods throughout northeastern Europe</p> <p>(2) Late winter floods around the North Sea and some sectors of the Mediterranean coast</p> <p>(3) Earlier winter floods in Western Europe.</p>

Seasonality analysis

Both trend and seasonality analysis	<i>Cunderlik and Ouarda (2009)</i>	Canada	<ul style="list-style-type: none"> (i) Sites: 162 streamflow records from relatively pristine and stable land-use conditioned watersheds (i) Period of analyses: 1974 to 2003 (ii) Data: Dominant Seasonal floods were analyzed (iii) Approach: The Mann–Kendall test in conjunction with the method of pre-whitening was used in the trend analysis and Directional statistics was used for seasonality analysis 	<ul style="list-style-type: none"> (1) The snowmelt floods shifted toward the earlier times of the year. (2) No significant trends were found in the timing of the rainfall dominated flood events. (3) The magnitude of the floods has been decreasing over the last three decades.
	<i>Burn et al. (2010)</i>	Canada	<ul style="list-style-type: none"> (i) Sites: 68 streamflow gauging stations in Canada (ii) Period of analyses: A record length of at least 50 years (1957–2006) (iii) Data: Extreme hydrological events (both high and low flows) drawn from annual and spring events (iv) Approach: Trends were analyzed using the Mann–Kendall test. A bootstrap resamplings-based field significance test was used to determine the <i>regional</i> trend. Seasonality measures that characterize the timing and persistence of extreme hydrologic events were examined using directional statistics 	<ul style="list-style-type: none"> (1) High flow events showed decreasing trends whereas low flow events showed both decreasing and increasing trends in flow magnitude. (2) Nival sites showed an earlier high flow occurrence and an earlier low flow occurrence. (3) Pluvial sites tend to experience a later annual maximum flow in the more recent part of the record.
	<i>Burn et al. (2016)</i>	Canada	<ul style="list-style-type: none"> (i) Sites: 132 gauging stations spread over Canada (ii) Period of analyses: Four periods ranging from 50 to 80 years (iii) Data: Peak over threshold (POT) dataset 	<ul style="list-style-type: none"> (1) There was an increased number of over threshold events. (2) There was increased importance of both rains on snow events and rainfall events

		(iv) Approach: Trend and Seasonality analysis were examined using the Mann–Kendall non-parametric test and directional statistics respectively.	and decreased importance of snowmelt events. (3) A transition of mixed flood regime to a more pluvial regime whereas nival catchments transition towards a more mixed response was observed.
<i>Matti et al. (2017)</i>	Scandinavia	(i) Sites: 59 catchments across Scandinavia (ii) Period of analyses: A record length of 54-122 years (1892–2014) (iii) Data: Seasonal maximum daily flows in a hydrological year (iv) Approach: Circular or directional statistics were used to assess flood seasonality and modified Mann–Kendall trend test was used for trend analysis	(1) Summer maximum daily flows showed a decreasing trend while winter and spring maximum daily flows showed an increasing trend (2) Snowmelt-dominated regime is shifting towards rainfall-dominated with consistent changes towards earlier flood peaks
<i>Burn and Whitfield (2018)</i>	Canada and the northern United States	(i) Sites: Hydrometric reference streamflow gauging stations at 27 natural watersheds (ii) Period of analyses: Past 100 years record span from 1916 to 2015 (iii) Data: Only POT time series (iv) Approach: Circular statistics were used to explore changes in the nature of the flood regime, Mann-Kendall non-parametric test was used for trend detection, and block bootstrap resamplings was used to correct for serial correlation in the data	(1) All flood regime show an increased number of threshold exceeding events. (2) A shift in the nival flood regime to a mixed regime and mixed flood regime to a pluvial regime is noted.

Change Point Analysis	<i>Villarini et al. (2009)</i>	The continental United States	<ul style="list-style-type: none"> (i) Sites: 50 stream gauging stations (ii) Period of analyses: Varying length for different stations with at least 100 years record starting from 1838 (iii) Data: Annual maximum peak discharge. (iv) Approach: A nonparametric Pettitt test was performed to detect abrupt changes in mean and variance of peak flows 	<ul style="list-style-type: none"> (1) 18 and 6 out of 50 stations exhibited a significant abrupt change in the mean and variance respectively. (2) Land use and land cover changes and gauge height variations have led to change points.
	<i>Nka et al. (2015)</i>	West Africa	<ul style="list-style-type: none"> (i) Sites: 11 catchments across West Africa (ii) Period of analyses: 1950-2010 (iii) Data: Annual maximum and POT series (iv) Approach: The Pettitt test was used to identify change points in the data 	<ul style="list-style-type: none"> (1) Most of the change points lie between 1950 and 2000 (2) Land use changes are the primary contributing factor for the change in flood magnitude.
In our study*	<i>This study</i>	Mahanadi River Basin, India	<ul style="list-style-type: none"> (i) Number of sites: 24 gauge stations (ii) Analyses period: varies between 1971 and 2016 (iii) Flood Event Samplings: Both Monsoon maximum series (MMPD) and peak over threshold (POT) series (iv) Approach: <ul style="list-style-type: none"> (a) Trend Detection: Mann-Kendall trend statistics to analyze monotonic trends and Pettitt change point statistics to identify abrupt shifts in the peak discharge time series. Field significance test was conducted to investigate the nature of the regional trend. 	<ul style="list-style-type: none"> (1) POT events showed increasing trend while MMPD events showed a mixture of increasing and decreasing trends in the middle reach (2) Mean date of peak discharge for all the sites was found during August (3) Delayed floods at lower reaches of Mahanadi River Basin

-
- (b) Seasonality analyses: using directional statistics.
 - (c) Change in timing of flood: Adjusted Theil-Sen slope estimator as employed in Bloschl et al. (2017)
-

*Contributions of current paper is added for the completeness

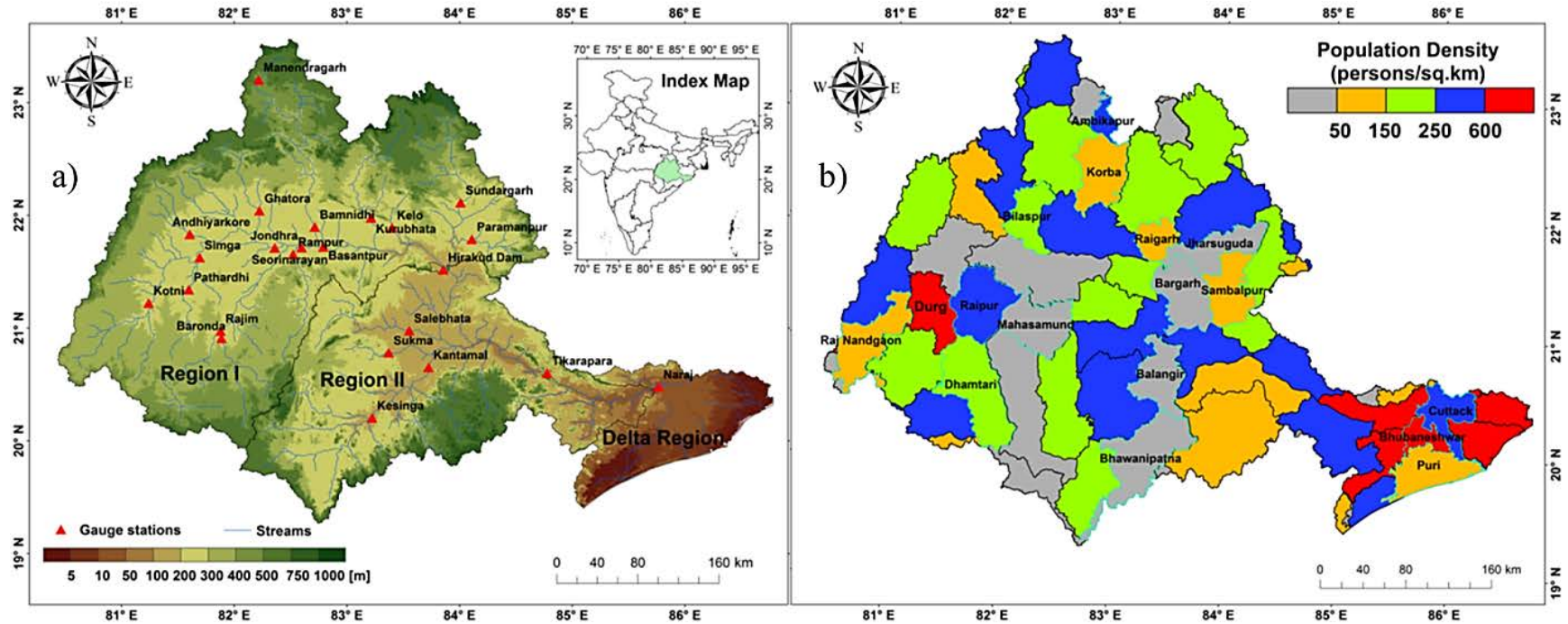


Fig. 1. Mahanadi river basin (a) Elevation map (b) District wise population density with highlighting major cities (Census data 2011).

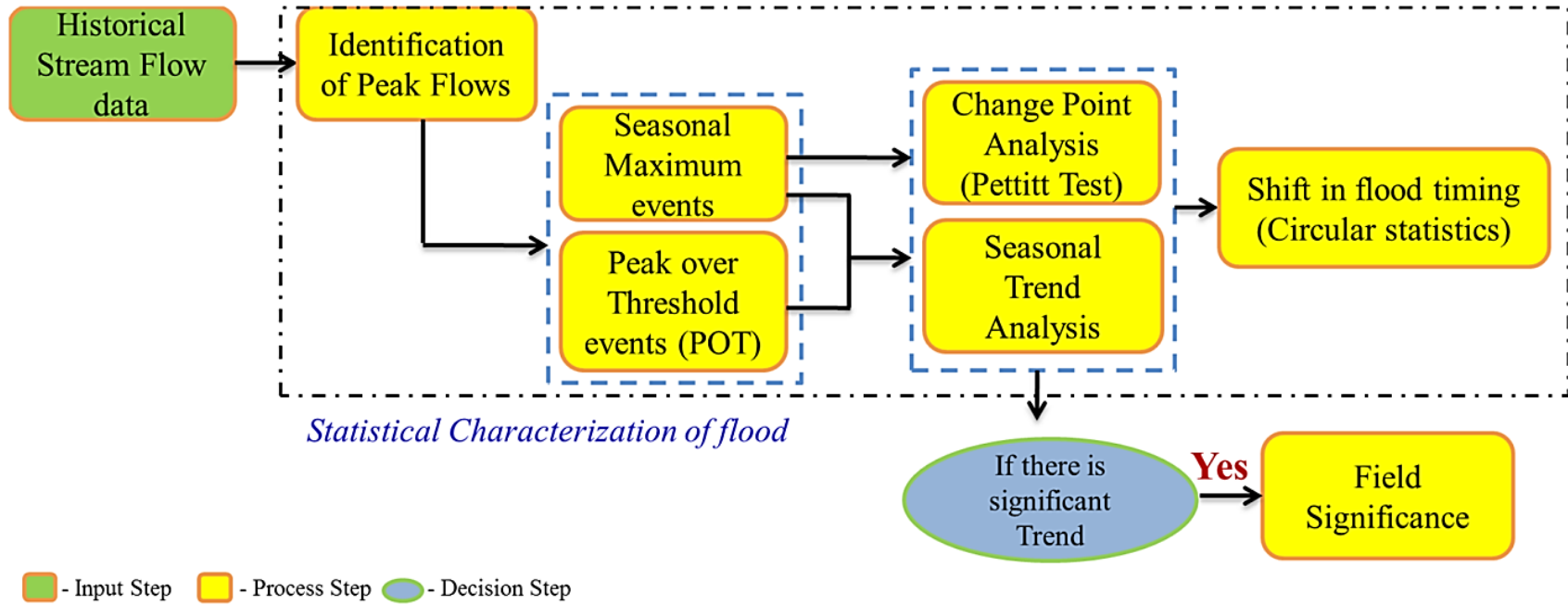


Fig.2. Flowchart summarizing the workflow.

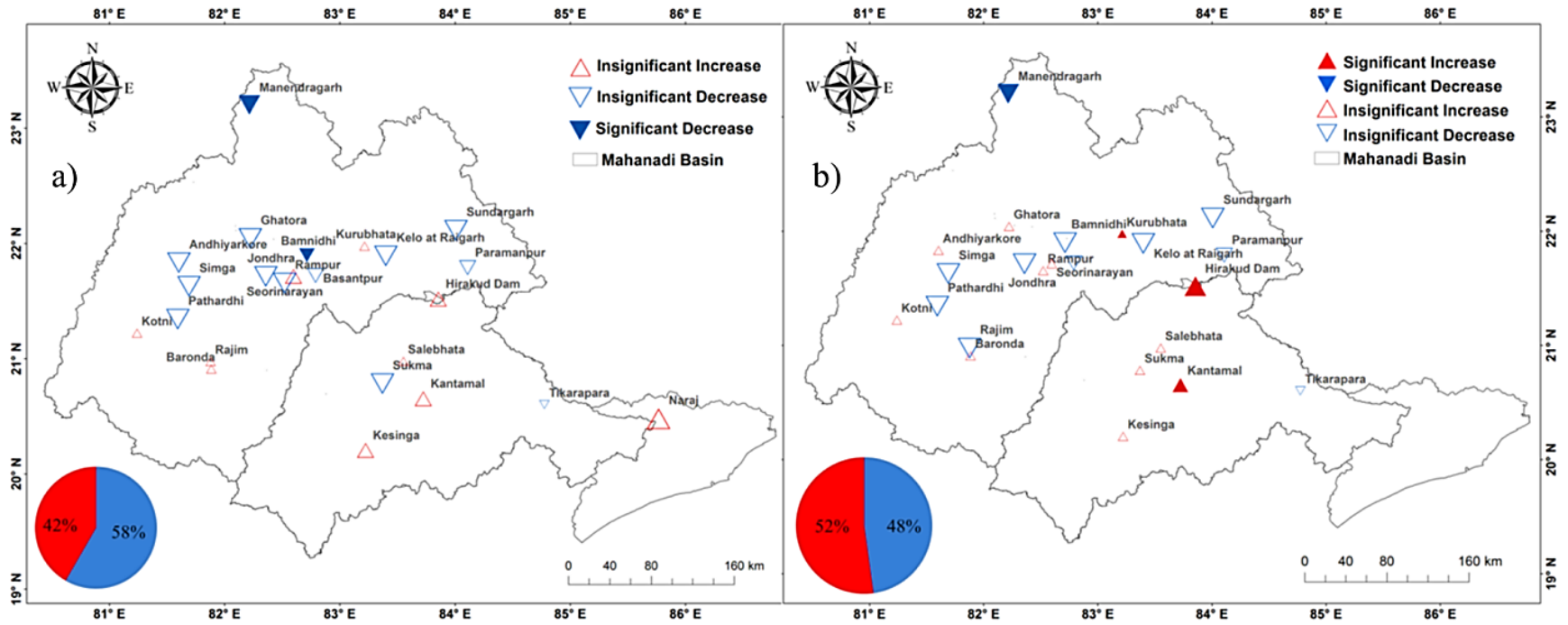


Fig. 3. Spatial trends at the 10% significance level (a) MMPD events and (b) POT events. The size of a triangle is proportional to the magnitude of trends calculated by the Theil Sen slope estimator.

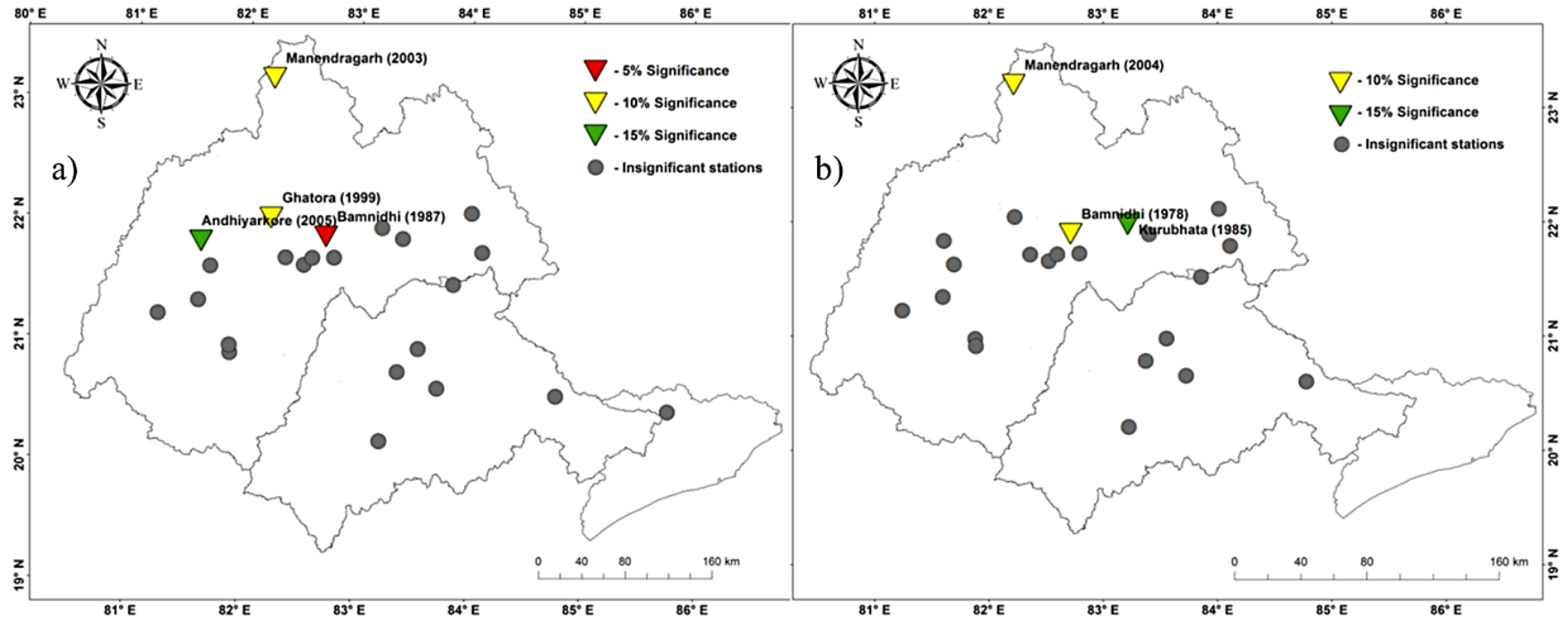


Fig. 4. Change point analysis (Pettitt test) of (a) MMPD events and (b) POT events for gauge stations at a significance level of 5, 10 and 15%, respectively. While the single change point analysis is performed by the Pettitt test, differences in mean stream flow after and before the detected change points are shown using the triangle. The downward orientation of the triangle indicates a decrease in mean stream flow after change point years at respective gauge location.

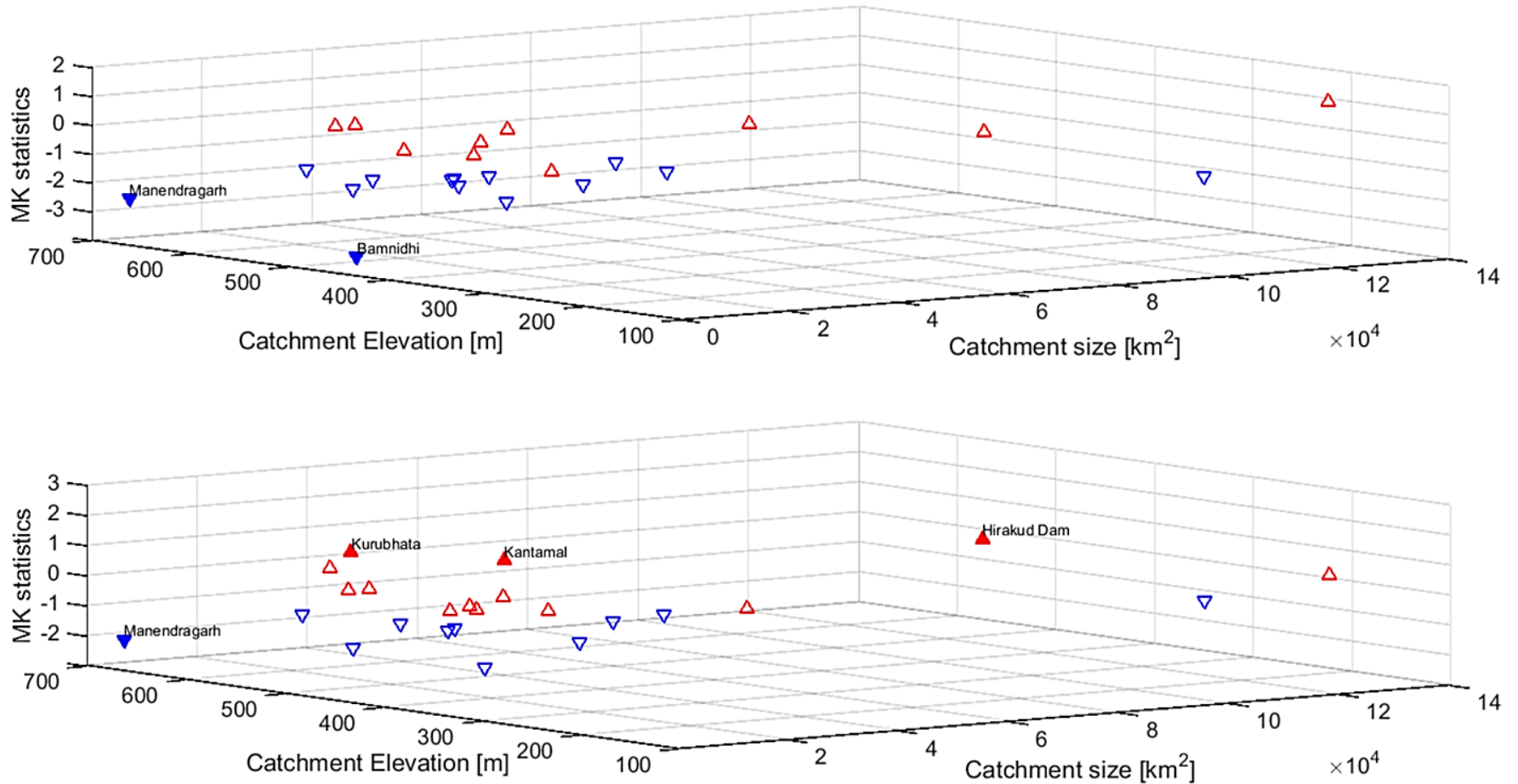


Fig. 5. Scale dependency relative to flood trends of MMPD events (*upper panel*) and POT events (*lower panel*). Mann-Kendall trend statistics are plotted as a function of the Catchment size (in km²) and Catchment elevation (in m). Shaded triangles indicate significant changes at the 10% significance level.

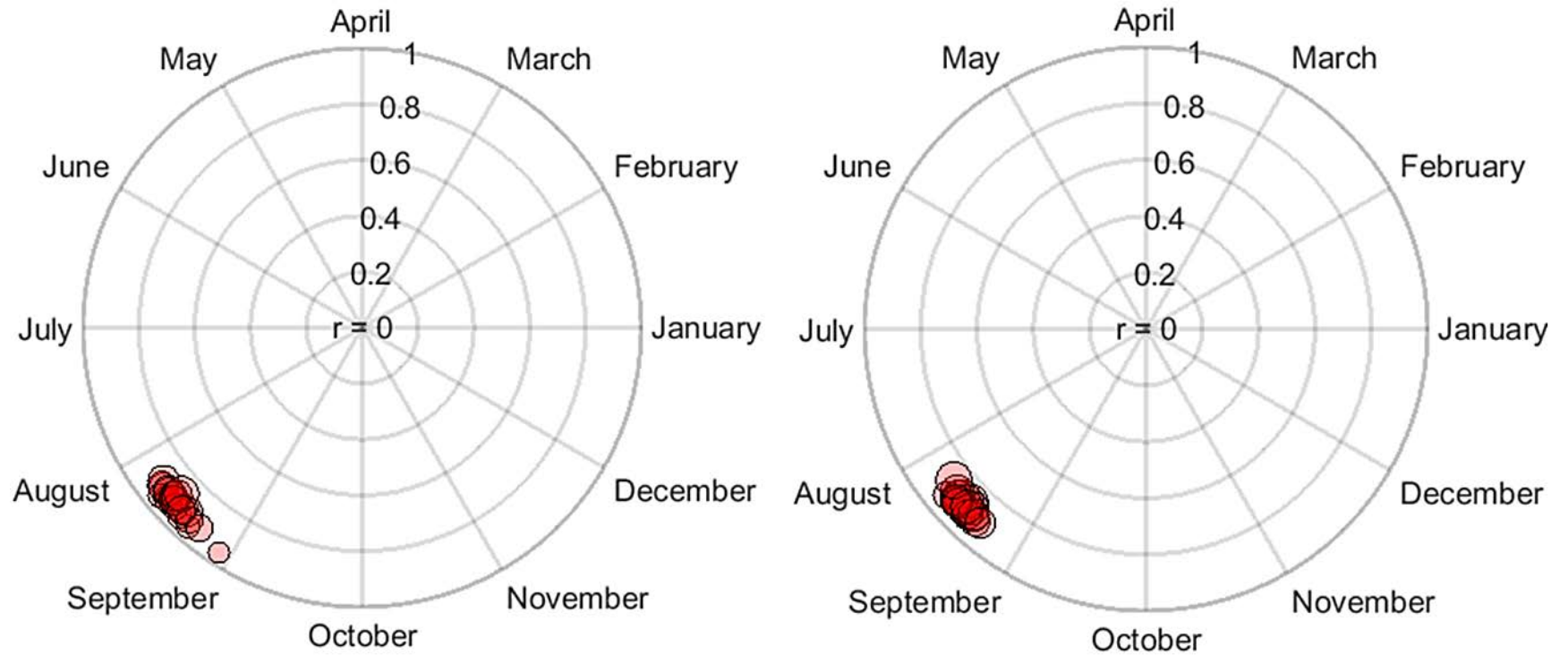


Fig. 6. The circular plots of mean date and persistence of floods using (*left panel*) MMPD and (*right panel*) POT events. The size of the circle indicates the value of circular variance with larger (smaller) size indicates a larger (smaller) variance.

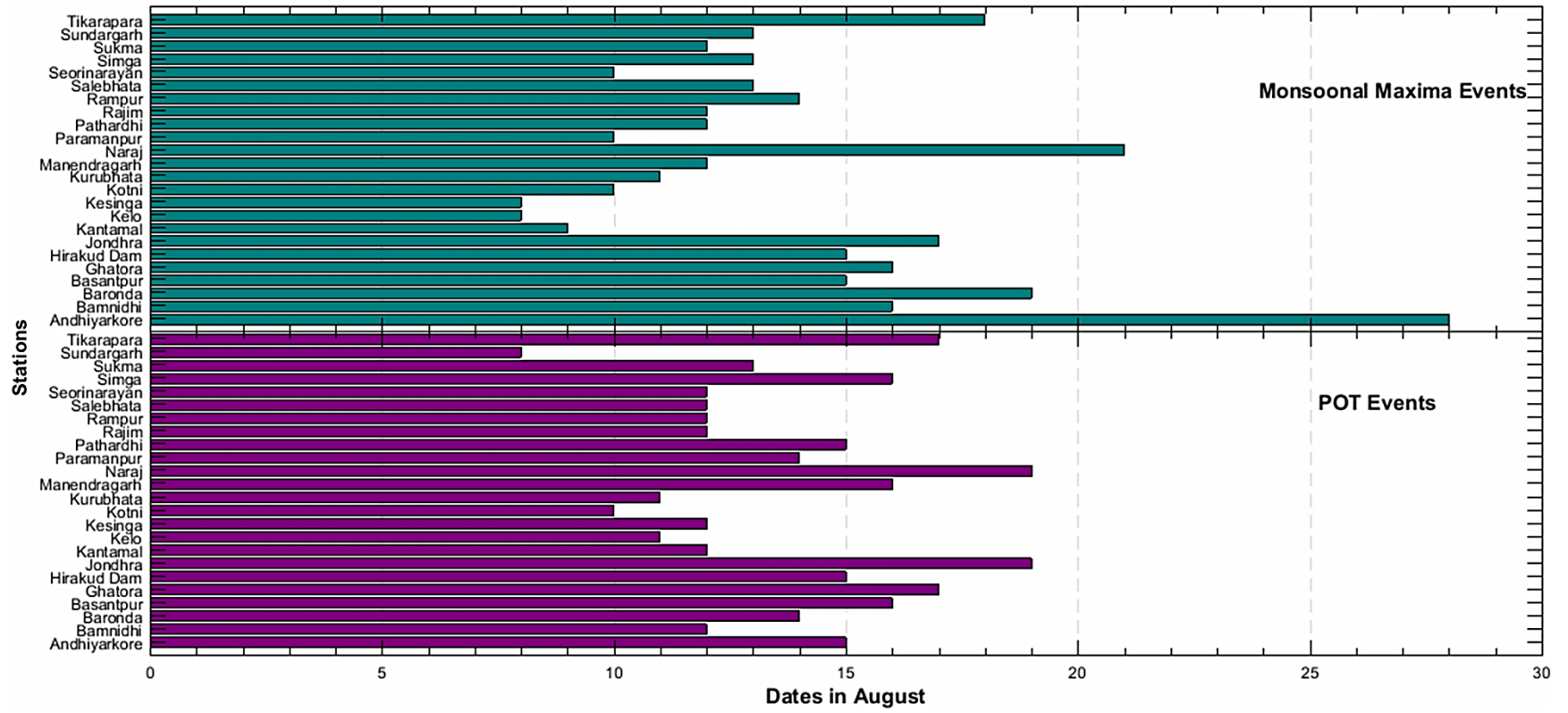


Fig. 7. Mean occurrence dates of Monsoonal Peak Discharge (MMPD) and Peak over Threshold (POT) flood events.

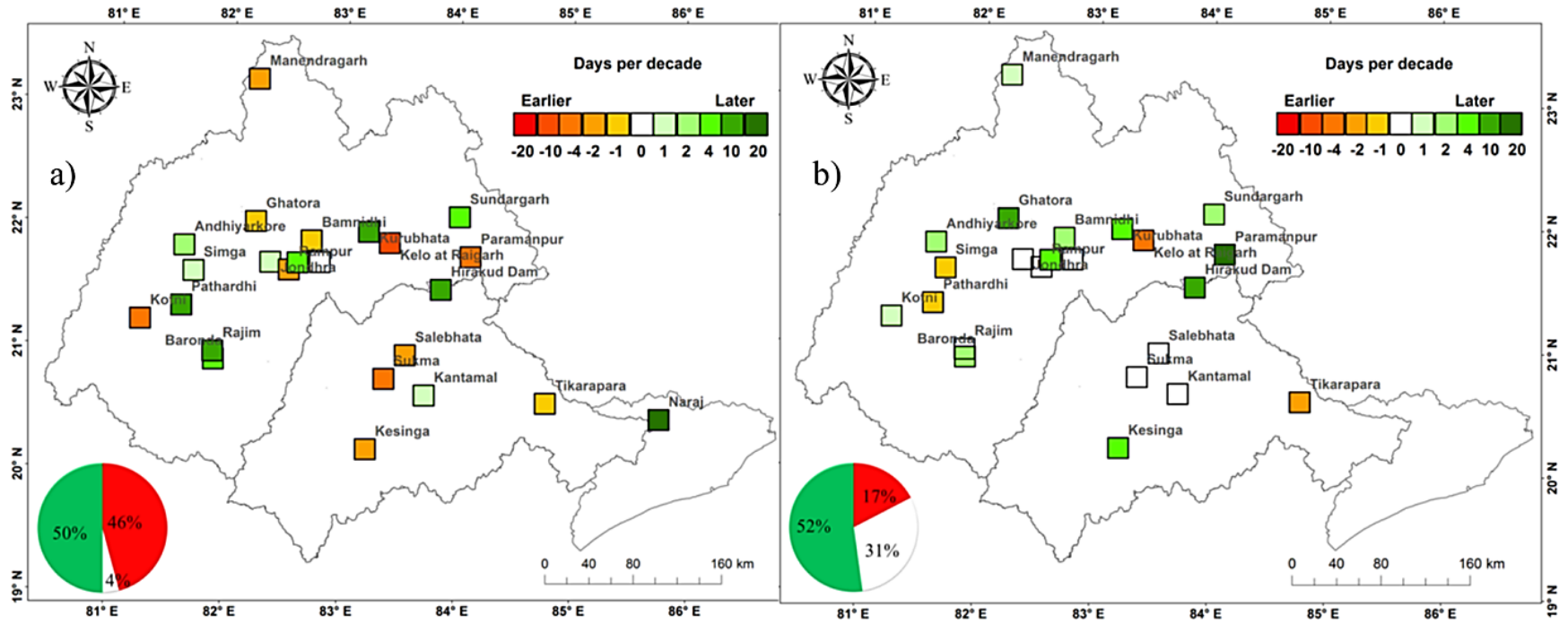


Fig. 8. Trends in flood timing of (a) MMPD events and (b) POT events at individual gauge stations. The shift in the date of flood occurrences is calculated in days per decade.